Structural investigations of Y substituted cobalt zinc ferrite by auto combustion method

K.K. Patankar [1#]Jyoti V. Devkar[1], Deepesh S. More[1] and V.L. Mathe [2]

1 Department of Physics, Rajaram College, Kolhapur 416004, India
2 Department of Physics, Savitribai Phule Pune University, Pune 411 007, India
 # Corresponding author email : ketaki.p30@gov.in

ABSTRACT

Rare earth doped ferrites are popular in transducer applications. The magnetostriction drastically changes on substituting transition metal ion with rare earth ion. However, synthesizing the rare earth doped spinel ferrite in itself is challenging due to the inevitable secondary phase. In this view, the present paper communicates successful synthesis of spinel ferrites with generic formula $Co_{0.8}Fe_{2-x}Zn_{0.2}Y_xO_4$ prepared by auto combustion technique. Structural analysis with various experimental techniques was carried out to confirm the successful synthesis of ferrite. XRD data shows spinel cubic single phase formation. Lattice constant and crystallite size were calculated using XRD data. Williamson-Hall plot shows strain in the sample. Morphological studies of the samples were recorded using scanning electron microscope. Compositional stoichiometry was confirmed from energy dispersive analysis of X-ray (EDAX) technique. Infrared absorption spectroscopy measurements were done in the frequency range of 400 cm^{-1} to 4000 cm^{-1}. Experimental results reveal the presence of splitting in the absorption band due to the presence of some ferrous ions. Two absorption bands were observed, in which strong absorption band corresponds to the metal oxygen vibration at tetrahedral sites and weak band to that of the octahedral sites. All these techniques together confirm the successful synthesis of rare earth doped ferrites.

Keywords: Ferrites; XRD; FTIR; Strain; Rare earth ion.

1. INTRODUCTION

Nanoferrite materials with different substitutions in the parent element magnetite ($FeO.Fe_2O_3$) have ubiquitous applications in all the fields beneficial to the mankind[1-8]. Out of the well-known nanoferrites, cobalt based ferrite has a special place in technological developments [9-13]. It is because of its properties such as high density, high memory storage capacity, high resistivity, squareness of the hysteresis loop, high Curie temperature and its low cost [11-13]. The properties possessed by these ferrites depend upon their chemical composition

and cation distribution at tetrahedral A-sites and octahedral B- sites [13]. Hence, proper substitution at both A and B sites leads to tailoring of magnetic properties. The Co-Zn ferrites are also significant materials and have been studied by many researchers using different techniques of synthesis [12, 14-19]. Analysis of the result shows that the 0.2 atomic level doping of Zn enhances magnetic saturation as well as resistivity. Rare earth substitution in ferrite also leads to remarkable change in magnetic properties due to the interactions between 3d-4f orbitals [20-23].

In ferrites, the distribution of the different ions at the tetrahedral and octahedral sites of the spinel lattice depends on the diameter of ions and the method of synthesis. Various physical and chemical methods of synthesis like chemical co precipitation, sol-gel, high energy ball milling, hydrothermal, citrate precursor, mechanical alloying, chemical combustion route and others have been developed to get nano ferrites. Amongst all these methods, chemical auto combustion is most suitable because of its simplicity, better control on particle size and other properties of materials [11-13]. Nano ferrite particles have been already synthesized by auto combustion method by many researchers [7,8, 11-13].

The doping of non magnetic rare earth ion in place of transition metal ion is quite challenging [11, 19]. It has resulted in inevitable secondary phase like R_2O_3 [20-23]. Moreover, the secondary phase deteriorating the magnetic properties is also well known. Therefore a limit on doping concentration must be properly tailored for successful synthesis of these materials. On the contrary, even with the inevitable secondary phase, the ferrites with rare earth doping have shown interesting magnetic properties. The authors attribute these peculiar magnetic behavior to the 3d-4f orbital interaction in ferrites [20-23]. The orbital interactions also lead to dramatic changes in magnetostriction, which is an inherent property of ferrites.

The structural characterization with techniques like XRD and IR are essential to rule out the secondary phase formation. These techniques are popular for giving finger prints of the material. The authentication of the desired stoichiometry is done only by using EDAX technique. The functionality of the material depends upon its microstructure development during the synthesis. This can be analysed by Scanning Electron Microscopy. Hence, the prepared ferrites were analysed for structural details through these techniques.

In this view, this paper intends to communicate the synthesis and structural studies of Yttrium doped cobalt Zinc ferrite.

2. EXPERIMENTAL TECHNIQUES

Synthesis: Nanocrystalline powders of yttrium doped cobalt zinc ferrites were prepared by auto combustion method. The A.R. grade citric acid ($C_6H_8O_7.H_2O$), cobalt ferrite ($Co(NO_3)_2.6H_2O$), zinc nitrate ($Zn(NO_3)_2.6H_2O$) ferric nitrate ($Fe(NO_3)_2.9H_2O$) and yttrium nitrate ($Y(NO_3)_3.6H_2O$) were used as initial ingredients. (>99% SD fine).The stoichiometric proportions of the nitrates and citric acid were weighed and added in 100 ml double distilled water to produce aqueous solution. The solution was kept on magnetic stirrer to form completely

dissolved solution. The ammonia solution was slowly added to adjust the PH to 7. Reaction procedure was carried out in the air atmosphere. Then continuous stirring and heating of mixed solution was initiated. During the chemical process, fumes of nitrates were released, then finally a very viscous black brown gel was formed.

The viscous gel was transferred on the hot plate. All water molecules are removed from the mixture and then the gel began to froth. After few minutes, the gel got automatically ignited and bursted with glowing flints. The ignition was completed within a minute yielding the brown colored ash termed as a precursor, which is the end product obtained by combustion method. The as prepared green powders of all the samples were sintered at 600^0 c for 8 hours to get the final product.

Characterization: The structural details were confirmed by X-ray diffraction(PW 1710 model), Fourier Transform Infrared spectroscopy(JASCO 6100 model), Scanning Electron Microscopy and Elemental Dispersive analysis technique.(JEOL JSM 6360 A).

Crystal structure and phase purity of the powders were investigated by using Cu-Kα radiations of wavelength 1.5418 A^0.The phase analysis was carried out by matching present data with the standard JCPDS card number 221086.

3. RESULTS AND DISCUSSION

3.1 XRD:Phase confirmation

Fig.1 shows the XRD pattern of $CoFe_{2-x}Zn_{0.2}Y_xO_4$ with (x =0.00, 0.01, 0.02, 0.03) The XRD pattern of the compound shows single phase formation as well as nanocrystalline nature. All the peaks observed for the oxides correspond to the spinel ferrite structure. As aforesaid indexing was done using JCPDScard number 221086.

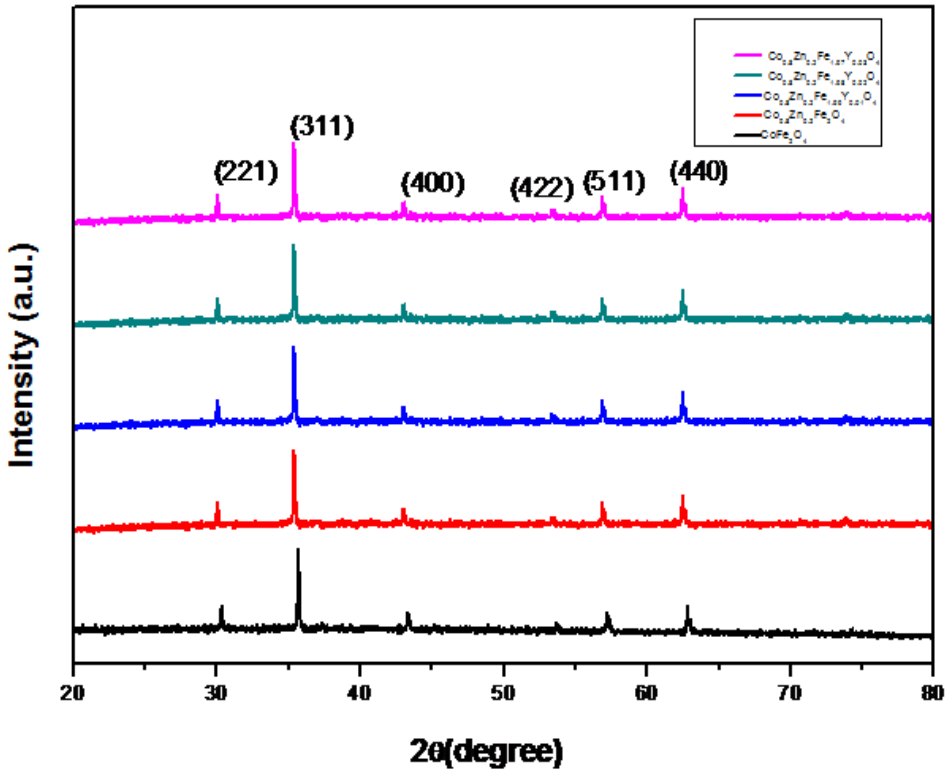

Fig.1. The XRD pattern of $CoFe_{2-x}Zn_{0.2}Y_xO_4$ with (x =0.00, 0.01, 0.02, 0.03)

The lattice constant'a' was determined using the following relation.

$a=d\sqrt{h^2+k^2+l^2}$ ----------(1)

Here, (h k l) are the Miller indices and d is the inter-planar spacing.

The average particle size was calculated using the Scherrer equation

$$D = \frac{0.9\lambda}{\beta \cos\theta} \quad \text{----------(2)}$$

Here, D is crystallite size, λ is the wavelength of X-ray radiation, θ is Bragg's angle, and β is the line width at half of the maximum height [24].

The Williamson – Hall plot works on the principle that the approximate formulae for size broadening, β_L, and strain broadening, β_e , vary quite differently with respect to Bragg angle, θ:

$$\beta_L = \frac{\mathbf{K}\lambda}{L\cos\theta}$$

$$\beta_e = \mathbf{C}\varepsilon\tan\theta$$

$$\beta_{tot} = \beta_e + \beta_L = \mathbf{C}\varepsilon\tan\theta + \frac{\mathbf{K}\lambda}{L\cos\theta}$$

If we multiply this equation by cosθ we get:

$$\beta_{tot}\cos\theta = \mathbf{C}\varepsilon\sin\theta + \frac{\mathbf{K}\lambda}{L}$$

This equation resembles the standard equation of straight line (y = mx + C). From this equation the particle size L is obtained from slope and strain is derived from the intercept.

From the figures 2 and 3, it is noted that the lattice parameter and the crystallite size increase with increase in doping percentage of yttrium. It is obvious as the ionic radius of rare earth ion (radius of Yttrium ion 1.02 Å) is greater than the iron ion(radius of ferric ion is 0.63 Å). Similar are the trends in variation for other rare earth doped ferrites [25 -27].

The lattice strain was calculated using Williamson-Hall plot. Fig.4 shows W-H plots for Y doped cobalt zinc ferrite. Fig.5 shows the variation of strain in ferrites for different levels of Y doping. The lattice parameter, crystallite size and Lattice strain, all these quantities increase with increase in Yttrium concentration. The values are tabulated in Table 1. Similar are the variations in Chromium substituted Co-Zn ferrites [28,29].

The variation of lattice parameter, crystallite size and strain in the samples with rare earth doping content have exact one is to one correspondence with each other. This is due to the substitution of higher ionic radius ion in the host lattices causes lattice strain. This is because the host lattice reserves specific interstitial volume to accommodate tetrahedral and octrahedral cations. If this volume is required to be replaced by volume of higher ionic radius, then automatically strain is induced in the surrounding lattice. This in turn causes increase in dimension of crystallite. It is obvious that the lattice parameter, size and strain in the samples to increase with increase in rare earth doping.

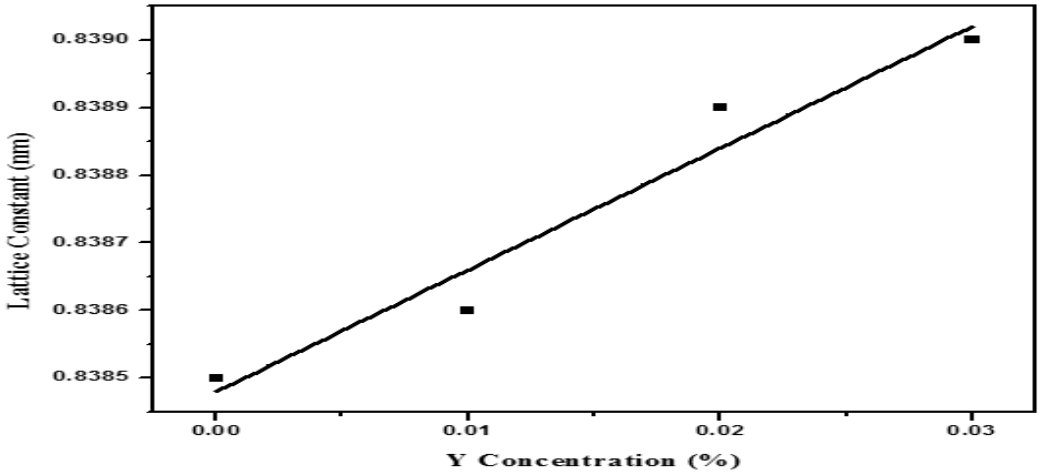

Fig.2 Variation of lattice parameter with Y content.

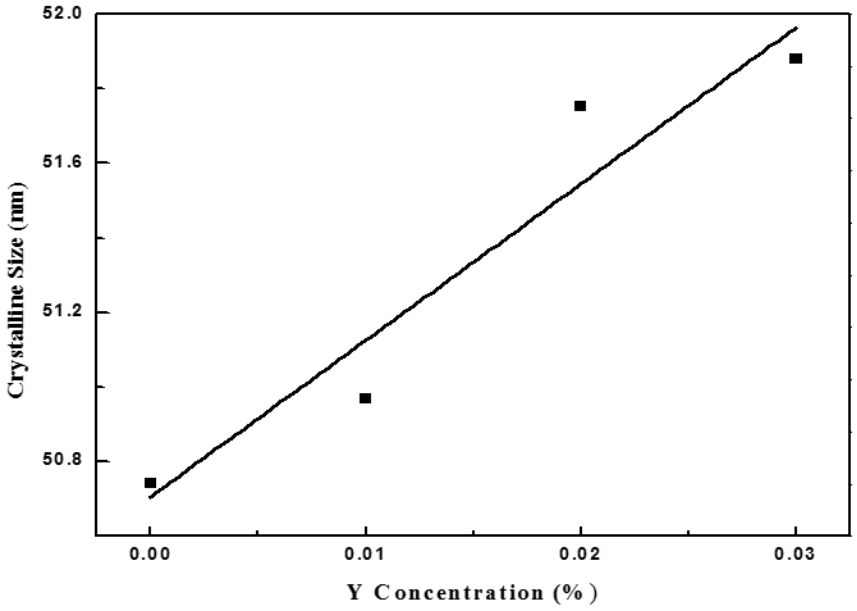

Fig.3 Variation of crystallite size with Yttrium content

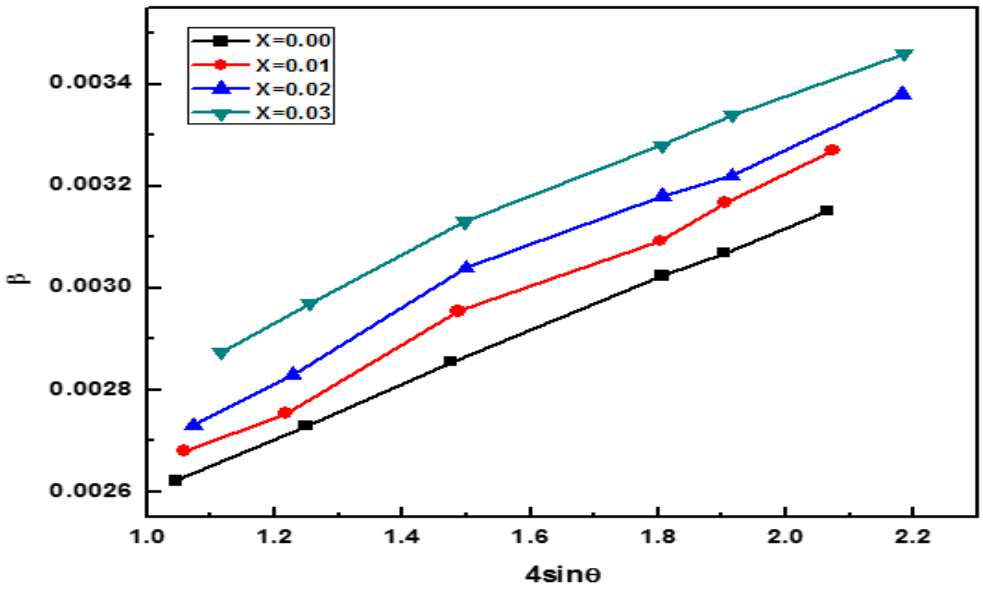

Fig.4 Williamson –Hall plots for $Co_{0.8}Zn_{0.2}Fe_{2-x}Y_xO_4$

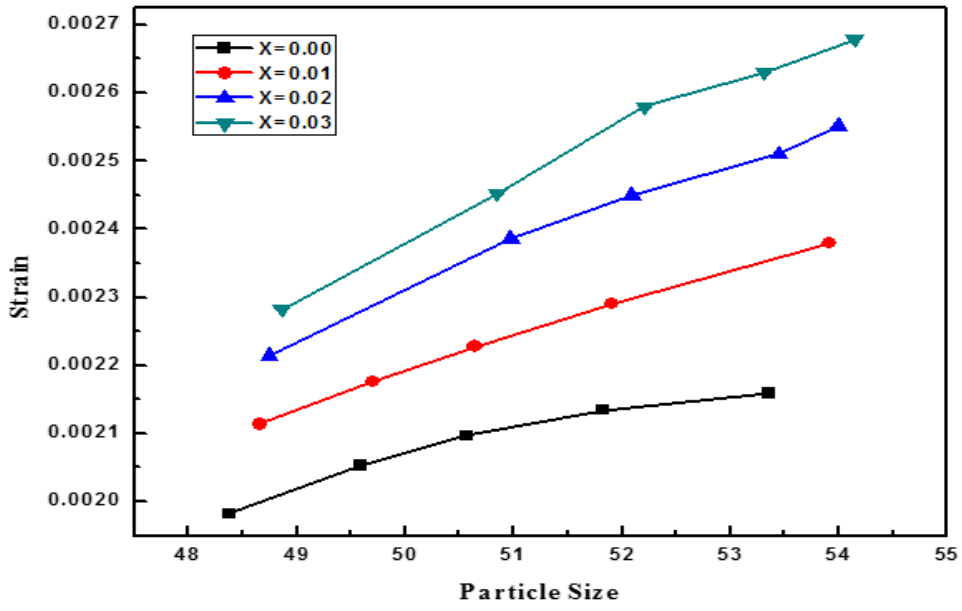

Fig.5 Variation of Strain with particle size for different Yttrium concentrations

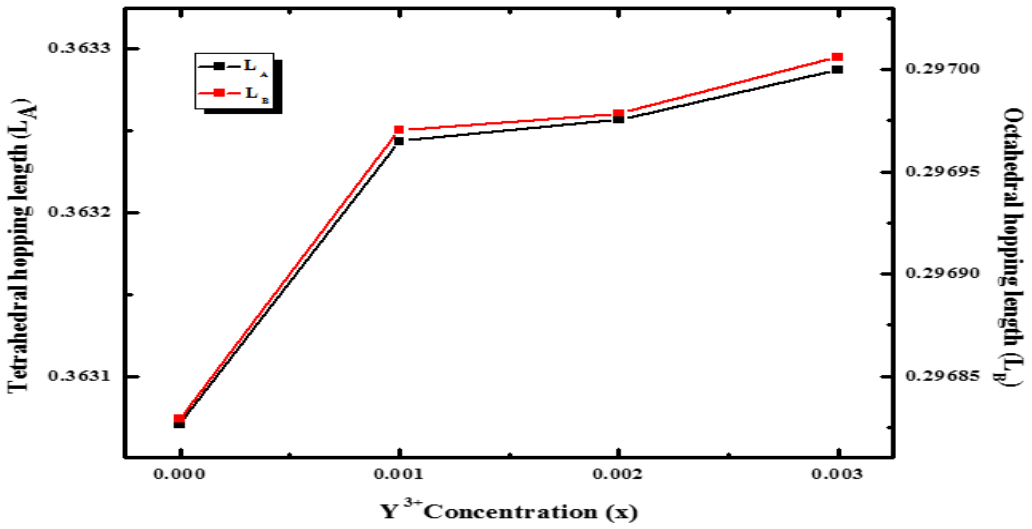

Fig.6 Variation of hopping length with Y^{+3} concentrations

The variations in the figures 2 – 5 are quite obvious due to the radius of Y^{+3} (1.02 Å) is greater than ionic radius of Ferric ion (0.63Å). Hence the hopping lengths at tetrahedral and octrahedral sites also show an increasing trend with increase in Y^{+3} content (Fig.6). Interestingly, a dramatic jump is obtained in the hopping lengths at A and B sites on yttrium substitution, which asserts inverse spinel structure of Co-Zn ferrite. However, the variation of Crystallite size (Fig.3) in the present case is unlike to variation in other rare earth doped ferrites [30-35]. The large ionic radius of rare earth ion causes lattice distortion because of which unit cell elongates and leads to increase in crystallite size. This also correlates to the increase in strain with increase in Yttrium content (Fig.5).

3.2 SEM

Fig.7 represents the SEM micrographs of the ferrite powders$CoFe_{2-x}Zn_{0.2}Y_xO_4$ with x =0.00, 0.01, 0.02, 0.03. The photographs show an aggregation of particles in yttrium doped samples only. The particles were observed as completely uniform grains in cobalt ferrite whereas partially uniform in cobalt zinc ferrite and agglomerated grains in rare earth doped cobalt zinc ferrite. However, nanoparticles were reflected in all the photographs. Similar is the picture in other rare earth doped ferrites [30-35]. The grain size calculated for each ferrite matches well with particle size data obtained from XRD. Magnetic interactions between various particles causes agglomeration. Intersetingly, agglomeration has increased with increase in Y content, eventhough ytttrium is non magnetic. This can be corelated to the site preferences of the various cations involved and their different types of magnetic interactions. It also requires magnetic studies for further jusification. The possibility lattice distortion causing creep and fatigue leading to agglomeration in grain orientation also cannot be ruled out.

$CoFe_2O_4$ $Co_{0.8}\ Zn_{0.2}O_4$

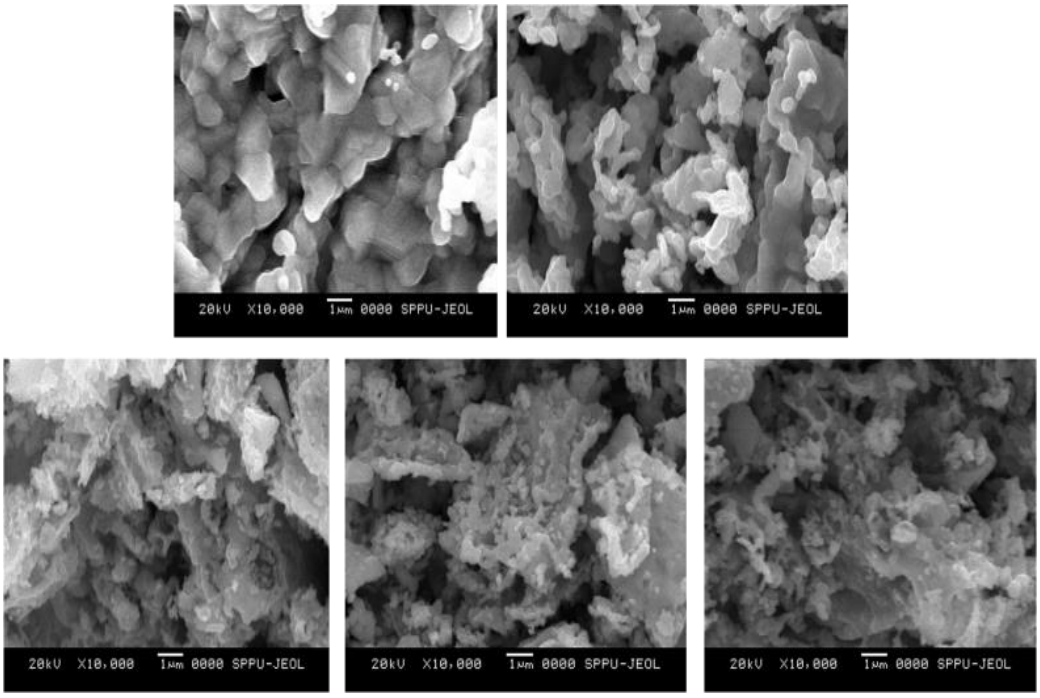

X=0.01 x= 0.02 x=0.03

Fig.7 SEM of **$Co_{0.8}Zn_{0.2}Fe_{2-x}Y_xO_4$**

3.3 Compositional analysis: EDAX

Fig.8 represents the compositional stoichiometry of typical $Co_{0.8}Zn_{0.2}Fe_{2-x}Y_xO_4$ ferrite nanoparticles. In the EDAX pattern, presence of Co^{2+}, $Fe3^{+}$, $Zn^{2+}$and O^{2}elements in proper proportions confirms the desired stoichiometry. The percentage of error of 2–3% is negligible. This error, though less significant, cannot be ruled out due to inevitable carbon content in combustion method of synthesis. Similar was reported in different materials synthesized by combustion route [36,37]. The EDAX results also confirm the precursors used for the synthesis have fully undergone the chemical reaction to form the single phase yttrium doped cobalt ferrites. This is significant result supporting the purity of compound and efficient doping of

foreign ion (Y^{+3}) in the host lattice $Co_{0.8}Zn_{0.2}Fe_2O_4$.

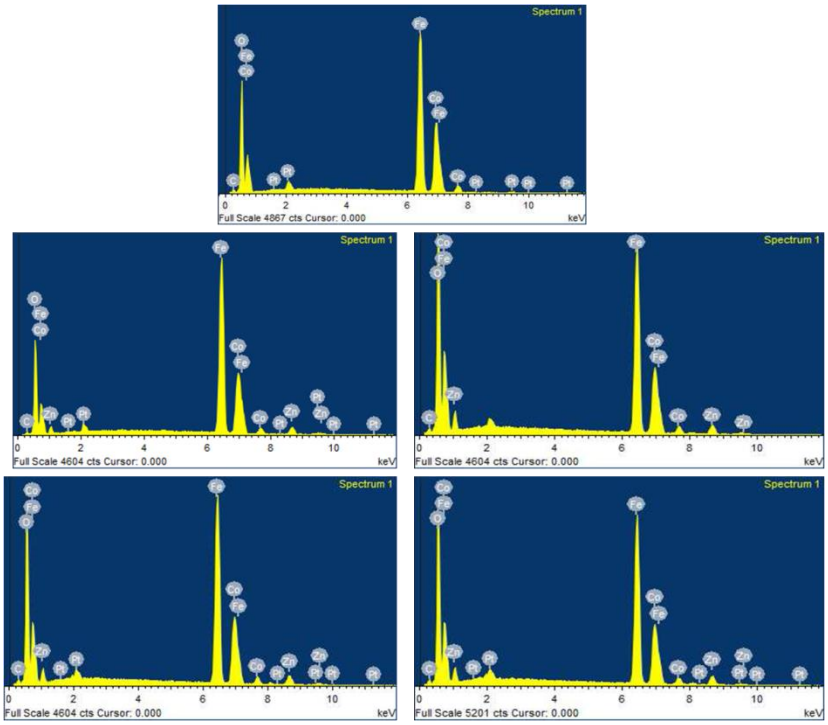

Fig .8 Energy dispersive analysis of X-ray spectrum (EDAX) of $CoFe_2O_4$ and $Co_{0.8}Zn_{0.2}Fe_{2-x}Y_xO_4$ ferrite (x=0,0.01, 0.02 and 0.03)

3.4 FTIR STUDIES

Fourier transform Infrared absorption spectroscopy provides position of ions in the crystal lattice as well as vibrational spectra. Infrared absorption spectra of samples were measured in the frequency range of 400 cm^{-1} and 4000cm^{-1} and are shown in Fig.9. All spinel ferrites consist two absorption bands because of the two different metals -oxygen stretching frequencies [38-40].

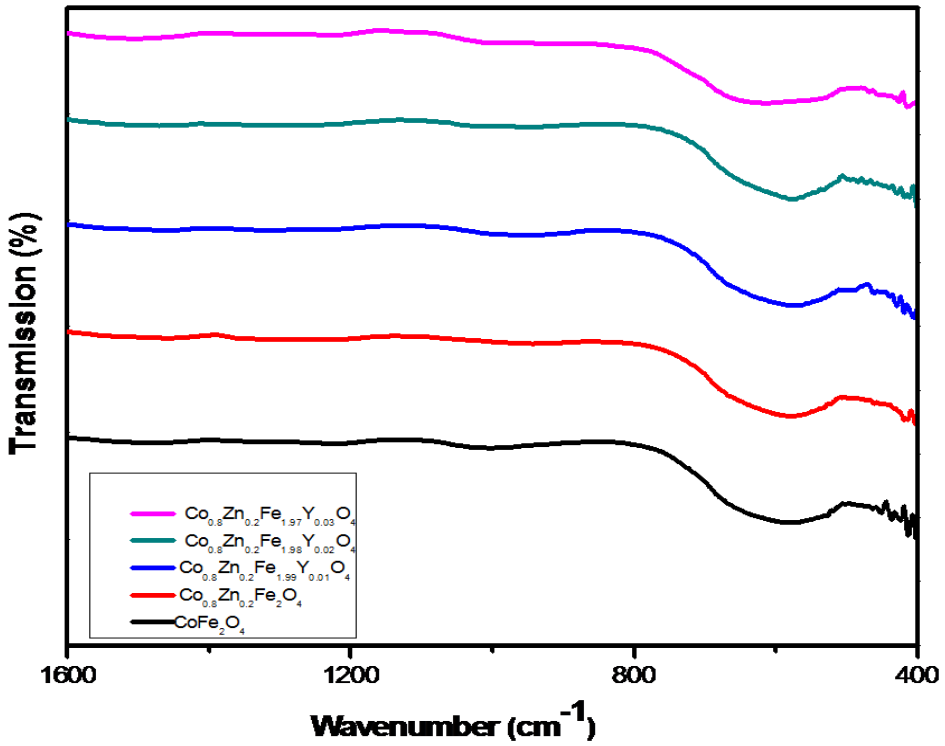

Fig.9 FTIR spectra of Yttrium doped Co-Zn ferrite series.

Two absorption band frequencies range in between 400-700cm^{-1}. The values of absorption band for all the samples are tabulated in Table 2. The table shows two main absorption bands at tetrahedral and octahedral sites and the threshold frequency of yttrium doped cobalt zinc ferrites. Out of the two absorption bands, one strong absorption band is obtained in the range of 560cm^{-1} to 585cm^{-1}. This band corresponds to tetrahedral complex in the ferrite structure. The second weak band ϑII appeared from 460cm^{-1}to 480 cm^{-1}, which corresponds to the octahedral complex of spinel ferrites. From these bands, it can be evinced that mode of vibration at the tetrahedral site is higher than that of mode of vibration at octahedral sites. It also accounts for strong absorption at tetrahedral complex than and weak absorption at octahedral complex. This is further attributed to the shorter bond length of tetrahedral sites than that of octahedral sites. The observed bands are in close agreement with the similar works on ferrites reported by other workers [38-40].

Interestingly, the strong band ϑI is attributed to the stretching of Fe3+ and O at the tetrahedral sites. It again gets splitted into three bands viz. with frequencies ϑ1(1),ϑ1 (2)and ϑ1(3). According to Potakawa, it is said that this type of splitting occurs only due to the presence of small amount of Fe2+ in the synthesized material[41]. This effect is considered as Jahn teller

distortion, which is produced by the presence of Fe2+ ions. The strain in the present samples is also confirmed from XRD studies.

In all, the local strain in the lattice on Y^{+3} doping ,as well as the presence of Jahn teller ion like Fe^{+2} ion make these material more suitable for magnetostrictive applications.

From the figure 9, It is observed that the threshold frequency is found out by noting the maximum point of absorption spectra, where it rise and attains a limiting value. When all the threshold frequencies of different samples are compared, the threshold frequency showed an increasing trend with the increase in Y content. The threshold energy is being calculated by the equation $E=h\vartheta$, where h is planks constant and ϑ is the threshold frequency. Thus substitution of Y also increases the threshold energy.

4. CONCLUSIONS

Nanocrystalline yttrium doped cobalt zinc ferrites were successfully synthesized by the auto-combustion technique using citric acid as a fuel. .X-ray diffraction results showed the formation of single phase cubic spinel structure. The increase in lattice constant, grain size, strain, hopping length confirms the flexibility in accommodation of non magnetic ion(Yttrium) in the host magnetic lattice despite mismatching of radii. EDAX confirms the desired stoichiometric proportions in all the samples. FTIR spectra show two absorptions bands near $400cm^{-1}$ and $600cm^{-1}$ characterizing the ferrite nature of the samples and also the presence of Jahn teller ion Fe^{+2}. The spontaneous strain developed suggests that the material is suitable for magnetostrictive applications. The structure of the material synthesized has to be thoroughly investigated before using it in any device. The structure determines the functionality or operating characteristics of the materials. It can also predict in which application the material is suitable. The present synthesized materials are suitable for transducer applications. Therefore, this paper communicates a detailed structural investigations of Y doped Co-Zn ferrites.

Acknowledgement*: We are grateful to UGC-DAE-CSR and University of Pune for suggestions and encouragement in carrying out this work.*

Funding : This work has been carried out without any funding from agencies.

Conflict of Interest: There is no conflict of interest amongst the authors. We together declare that there is no conflict of interest.

REFERENCES

1. *Yan Z, Gao J, Li Y, Zhang M et al (2015) , "Hydrothermal synthesis and structure evolution of metal-doped magnesium ferrite from saprolite laterite", RSC Adv ,5,92778–92787.*

2. *Latham AH, Williams ME (2008) "Controlling transport and chemical functionality of magnetic nanoparticles", Acc Chem Res, 41,411–420.*

3. Moussaoui HE, Mahfoud T, Habouti S et al (2016), " Synthesis and magnetic properties of tin spinel ferrites doped manganese", J Magn Magn Mater ,405,181–186.

4. Mathew DS, Juang R (2007),"An overview of the structure and magnetism of spinel ferritenanoparticles and their synthesis in micro emulsions", Chem Eng J 129, 51–65.

5. Carta D, Casula MF, Falqui A et al (2009), "A structural and magnetic investigation of theinversion degree in ferrite nanocrystals MFe2O4 (M : Mn, Co, Ni)", J Phys Chem C, 113, 8606–8615.

6. Song Q, Ding Y, Wang ZL et al (2007),"Tuning the thermal stability of molecular precursors for the nonhydrolytic synthesis of magnetic MnFe2O4spinel nanocrystals", Chem Mater ,19,4633–4638.

7. Kefeni KK, Msagati TAM, Mamba BB (2017),"Ferrite nanoparticles: synthesis, characterization and applications in electronic device", Mater Sci Eng B, 215, 37–55.

8. Pang YL, Lim S, Ong H et al (2016), "Research progress on iron oxide-based magnetic materials: synthesis techniques and photocatalytic applications. Ceram Int, 42, 9–34.

9. Goswami PP, Choudhury HA, Chakma S et al (2013), "Sonochemical synthesis and characterization of manganese ferrite nanoparticles", Ind Eng Chem Res, 52, 17848–17855.

10. Shobana MK, Nam W, Choe H, (2015),"Improved structural and magnetic properties of cobalt nanoferrites: Influence of sintering temperature", Ceramic International, Volume, April 2015,Pages 4492-4497.

11.Shobana MK, Nam W, Choe H, (2013),"Yttrium-doped cobalt nanoferrites prepared by sol-gel combustion method and its characterization",J Nanosci Nanotechnol., 2013 May, 13(5), 3535-8.

12. Ritu Rani, Gagan Kumar, Khalid Mujasam Batoo, M. Singh,(2013), "Electric and Dielectric Study of Zinc Substituted Cobalt Nanoferrites Prepared by Solution Combustion Method", American Journal of Nanomaterial's, 2013, Vol. 1, No. 1, 9-13.

13. Krutika L. Routray, Dhrubananda Behera,(2017), "Structural and Dielectric Properties of Bismuth Doped Cobalt Nano Ferrites Prepared by Sol-Gel Auto Combustion Method" IOP Conf. Series: Materials Science and Engineering, 178, 012007.

14.Juejin Ji, Zhenqian Zhang, Bijun Fang and Jianning Ding , (2017)"Preparation of Co–Zn ferrite nano-based materials and their enhanced magnetic performance via inverse miniemulsion method",Material Research Express, Volume 4, Number 11. 89-97.

15.Hyunkyung Choi,Sangjoon Lee,Taejoon Kouh,Sam Jin Kim, Chul Sung Kim,Eunjoo Hahn, "Synthesis and characterization of Co-Zn ferrite nanoparticles for application to magnetic hyperthermia", Journal of the Korean Physical Society, Volume 70, Issue 1, (2017),pp 89–92.

16.Tetiana Tatarchuk, Mohamed Bououdina, Wojciech Macyk,Olexander Shyichuk,Natalia Paliychuk, Ivan Yaremiy, Basma Al-Najar,and Michał Pacia, (2017),"Structural, Optical, and Magnetic Properties of Zn-Doped $CoFe_2O_4$ Nanoparticles",Nanoscale Res Lett., 12, 141-149.

17.A.R.Lamani, H.S.Jayanna, C.S.Naveen, M.P.Rajeeva and G.D.Prasanna,(2015),"Microwave Dielectric and Magnetic Properties of Co-Zn Ferrites", IOP Conf. Series: Materials Science and Engineering,73,012124 -29.

18. Rabia Qindeel ,(2018) , "Synthesis and characterization of Co-Zn based spinel ferrites",Materials Research Express, Volume 5, Number 8, 11-22.

19.Akhtar, Majid Niaz; Khan, Muhammad Azhar , "Effect of rare earth doping on the structuraland magnetic features of nanocrystalline spinel ferrites prepared via sol gel route",Journal of Magnetism and Magnetic Materials, Volume 460, p. 268-277.

20. AhmedM. A. & Ateia, Ebtesam & El-Dek, Samaa, (2003). Rare earth doping effect on the structural and electrical properties of Mg–Ti ferrite". Materials Letters, 57, 4256-4266.

21.CharalamposStergiou , (2017), Magnetic, dielectric and microwave absorption properties of rare earth doped Ni–Co and Ni–Co–Zn spinel ferrites. Journal of Magnetism and Magnetic Materials ,Volume 426, Pages 629-635.

22. X. C. Zhong, X. J. Guo, S. Y. Zou, H. Y. Yu, Z. W. Liu, Y. F. Zhang, and K. X. Wang, (2018)Improving soft magnetic properties of Mn-Zn ferrite by rare earth ions doping", AIP Advances ,8, 047807-12.

23.Qing Lin, Jinpei Lin, Yun He, Ruijun Wang and Jianghui Dong, (2014), "The Structural and Magnetic Properties of Gadolinium Doped CoFe2O4 Nanoferrites", Journal of Nanomaterials Volume 2015, Article ID 294239, 1-6.

24. S.T.Alone,SagarE.Shirsath, R.H.Kadam, K.M. Jadhav,(2011)Chemical synthesis, structural and magnetic properties of nano-structured Co–Zn–Fe–Cr ferrite, Journal ofAlloysandCompounds509(2011)5055–5060.

25. K. K. Patankar, D. M. Ghone, V. L. Mathe, S. D. Kaushik, Structural and physical property study of sol–gel synthesized $Co_{0.8}Zn_{0.2}$ $Fe_{2\_x}Ho_xO_4$ nano ferrites, Journal of Magnetism and Magnetic Materials 454 (2018) 71–77.

26. D.D. Sateesh Prathapani, M. Vinitha, T.V. Jayaraman, Effect of Er doping on Structural and magnetic properties of cobalt ferrite, J. Appl. Phys. 115 (2014), 17A502-12.

27. L. Ben Tahar, M. Artus, S. Ammar, L.S. Smiri, F. Herbstb, M.-J. Vaulay, V. Richard, J.-M. Grene`che, F. Villain, F. Fie´ vet, Magnetic properties of CoFe1.9RE0.1O4 nanoparticles (RE ¼ La, Ce, Nd, Sm, Eu,Gd, Tb, Ho) prepared in polyol , Journal of Magnetism and Magnetic Materials 320 (2008) 3242–3250.

28. S.T.Alone,SagarE.Shirsath, R.H.Kadam, K.M.Jadhav, Chemical synthesis, structural andmagneticpropertiesofnano-structuredCo–Zn–Fe–Crferrite,Journal of Alloys and Compounds 509 (2011) 5055–5060.

29. J. Peng, M. Hojamberdiev, Y. Xu, B. Cao, J. Wang, and H. Wu, "Hydrothermal synthesis and magnetic properties of gadolinium-doped CoFe2O4 nanoparticles," Journal of Magnetism and Magnetic Materials, vol. 323, no. 1, 2011, pp. 133–138.

30. Qing Lin, Jinpei Lin Yun He, Ruijun Wang and Jianghui Dong, "The Structural and Magnetic Properties of Gadolinium Doped CoFe2O4 Nanoferrites", Journal of Nanomaterials Volume 1,2015,1-6.

31 J. Jiang and Y.-M. Yang, "Effect of Gd substitution on structural and magnetic properties of Zn-Cu-Cr ferrites prepared by novel rheological technique," Materials Science and Technology, vol. 25, no. 3, 2009, pp. 415–418 .

32. Y. Y. Meng, Z. W. Liu, H. C. Dai et al., "Structure and magnetic properties of Mn(Zn)Fe2−xRExO4 ferrite nano-powders synthesized by co-precipitation and refluxing method," Powder Technology, vol. 229, 2012, pp. 270–275.

33. L. Zhao, Y. Cui, H. Yang, L. Yu, W. Jin, and S. Feng, "The magnetic properties of Ni0.7Mn0.3GdxFe2−xO4 ferrite," Materials Letters, vol. 60, no. 1, 2006,pp. 104–108.

34. M. Asif Iqbal, M.-U. Islam, M. N. Ashiq, I. Ali, A. Iftikhar, and H. M. Khan, "Effect of Gd-substitiution on physical and magnetic properties of Li1.2Mg0.4GdxFe(2–x)O4 ferrites," Journal of Alloys and Compounds, vol. 579,2013, pp. 181–186.

35. R. N. Panda, J. C. Shih, and T. S. Chin, "Magnetic properties of nano-crystalline Gd- or Pr-substituted CoFe2O4 synthesized by the citrate precursor technique," Journal of Magnetism and Magnetic Materials, vol. 257, no. 1,2003, pp. 79–863.

36. A.Manikandan, J.Judith Vijaya, L.John Kennedy, M.Bououdina, "Microwave combustion synthesis, structural, optical and magnetic properties of $Zn_{1-x}Sr_xFe_2O_4$ nanoparticles", Ceramics International Volume 39, Issue 5, July 2013, Pages 5909-5917.

37. Tagreed M. Al-Saadi1, Ahmed H.Abed , Ayad Ahmed Salih, "Synthesis and Characterization of AlyCu0.15Zn0.85-yFe2O4 Ferrite Prepared by the Sol-Gel Method", Int. J. Electrochem. Sci., 13 (2018) 8295 – 8302

38. D.D. Sateesh Prathapani, M. Vinitha, T.V. Jayaraman, Effect of Er doping onstructural and magnetic properties of cobalt ferrite, J. Appl. Phys. 115 (2014),17A,502-8.

39. S. A Mazen and T.A Elmosalami, "Structural and elastic properties of Li Ni ferrite, ISRN Condensed matter Physics, 2011, Article ID 820726, 2011,1-6.

40. M. Stefanescu, C. Caizer, M. Stoia, O.Stefanescu, "Ni, Zn/SiO2 ferrite nanocomposites prepared by an improved sol-gel method and their characterization", Journal of Optoelectronics and Advanced Materials Vol. 7,No.2, April 2005,607-614.

41 SANATOMBI SOROKHAIBAM, IBETOMBI SOIBAM, SUMITRA PHANJOUBAM, 'FTIR STUDIES OF COPPER SUBSTITUTED LITHIUM FERRITE PREPARED BY THE CITRATE PRECURSOR METHOD", International Journal of Advances in Science Engineering and Technology, Vol-4, Iss-3, Spl. Issue-1 Aug.-2016,120-122.

Sr. No.	Name of sample	Lattice constant (nm)	Crystalline size (nm)	Lattice strain
1	$CoFe_2O_4$	0.8383	50.35834	$2.21*10^{-3}$
2	$Co_{0.8}Zn_{0.2}Fe_2O_4$	0.8385	48.39825	$2.18*10^{-3}$
3	$Co_{0.8}Zn_{0.2}Fe_{1.99}Y_{0.01}O_4$	0.8389	48.64573	$2.127*10^{-3}$
4	$Co_{0.8}Zn_{0.2}Fe_{1.98}Y_{0.02}O_4$	0.8389	48.64573	$2.129*10^{-3}$
5	$Co_{0.8}Zn_{0.2}Fe_{1.97}Y_{0.03}O_4$	0.8390	53.42182	$2.17*10^{-3}$

Table 1 XRD data of $Co_{0.8}Zn_{0.2}Fe_{2-x}Y_xO_4$.

Sample	Tetrahedral sites Fe3+-O				Octahedral sites ϑ2	Threshold Frequency
	ϑ1(1)	ϑ1(2)	ϑ1	ϑ1 (3)		
$CoFe_2O_4$	740	679	583	544	461	788
$Co_{0.8}Zn_{0.2}Fe_2O_4$	736	674	575	540	469	780
$Co_{0.8}Zn_{0.2}Fe_{1.99}Y_{0.01}O_4$	731	667	567	536	471	767
$Co_{0.8}Zn_{0.2}Fe_{1.98}Y_{0.02}O_4$	726	663	566	533	476	752
$Co_{0.8}Zn_{0.2}Fe_{1.97}Y_{0.03}O_4$	712	651	562	529	480	744

Table 2 FTIR data of $Co_{0.8}Zn_{0.2}Fe_{2-x}Y_xO_4$